Best
Available
Copy
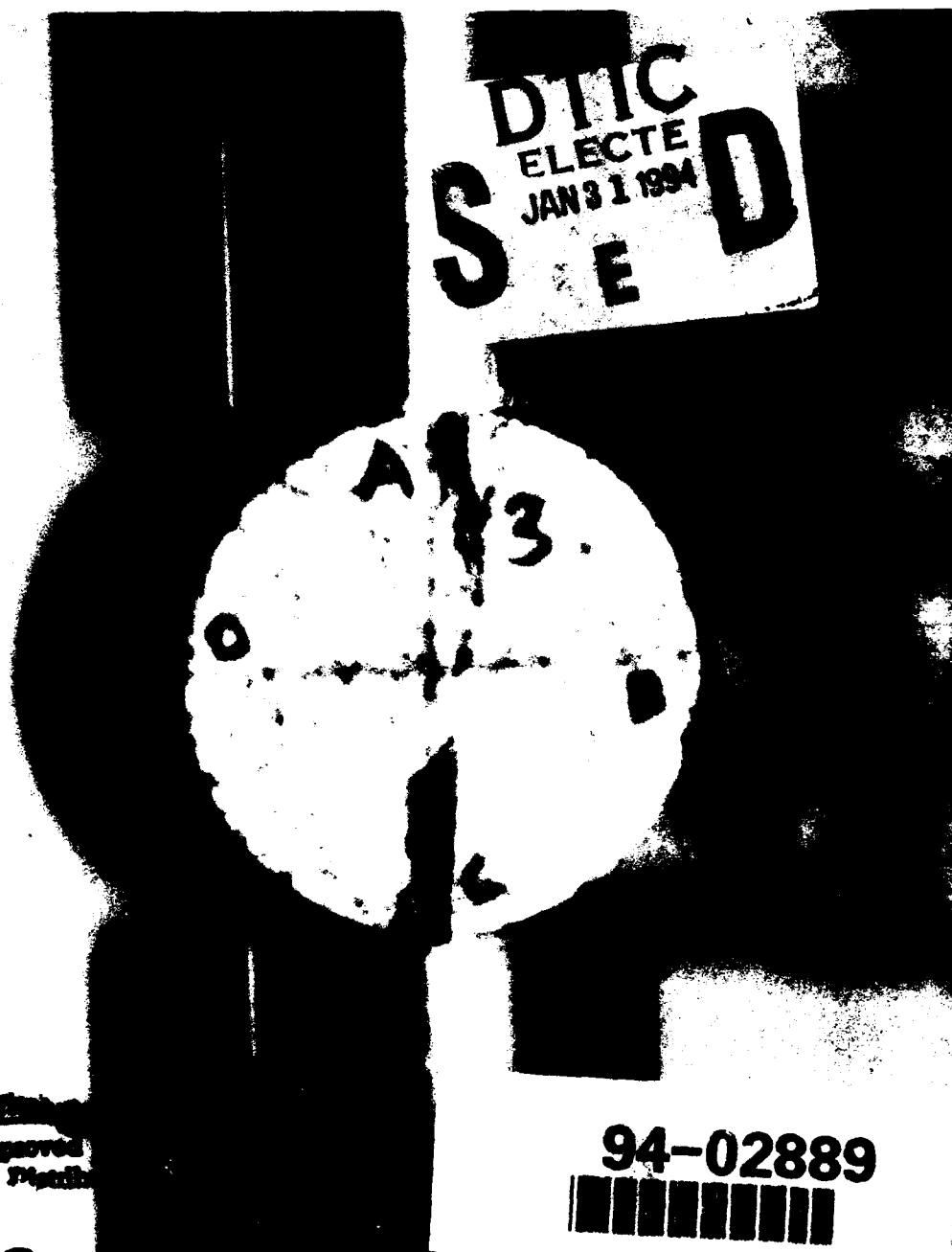
High-Strain-Rate Tensile Behavior of Sedimentary and Igneous Rocks at Low Temperatures

Piyush K. Dutta and Kunsoo Kim

October 1993

94-02889

Abstract

The influence of low temperature on the stress–strain behavior, fracture strength, and energy absorption in the dynamic fracturing of a limestone and a granite was determined by experiments conducted with a special low temperature split-Hopkinson pressure bar in the tensile strain rate regime of 80–100 strains s^{-1}. The tensile strength was determined by diametral compression of disk samples (Brazilian method) at –40°C and 24°C. Diametral strains to failure were monitored with a high-speed digital oscilloscope to observe deformations at microsecond intervals. These data were then compared with the results from room and low temperature quasi-static tests. Results show that the tensile strength and the deformability of these rocks are more sensitive to loading rate than to temperature. The mechanism of failure under dynamic loading by stress waves is significantly different from that under quasi-static loading. Dynamic loading produces multiple fractures, absorbs more energy and, because of the cushion of broken rocks produced under the loading surface, requires higher loads for complete failure. The influence of low temperature on strength and deformability under both static and dynamic loadings is less dramatic. Nevertheless, in all cases the strength increased with decreasing temperatures, possibly because of the immobilization of the interfacial water below the freezing temperature.

Cover: Granite sample tested in Hopkinson
bar. (Photo by R. Demars.)

CRREL Report 93-16

**U.S. Army Corps
of Engineers**
Cold Regions Research &
Engineering Laboratory

High-Strain-Rate Tensile Behavior of Sedimentary and Igneous Rocks at Low Temperatures

Piyush K. Dutta and Kunsoo Kim   October 1993

Accesion For

NTIS CRA&I	☑	
DTIC TAB	☐	
U..announced	☐	
Justification		

By ....
Di.t.ibution /

Availability Codes

Dist	Avail and / or Special
A-1	

PREFACE

The contents of this report are not to be used for advertising or promotional purposes. Citation of brand names does not constitute an official endorsement or approval of the use of such commercial products.

High-Strain-Rate Tensile Behavior of Sedimentary and Igneous Rocks at Low Temperatures

PIYUSH K. DUTTA AND KUNSOO KIM

INTRODUCTION

The aim of this study was to develop a better understanding of the mechanics of fragmentation of rocks in impact crushing at low temperatures. The effect of low temperature on mechanical properties of hard rocks has received relatively little attention although there is a general belief that rock becomes stronger when cold. Mellor (1971, 1973) studied the stress-strain behavior for air-dry and saturated rocks of several types and observed that both compressive and tensile moduli and both compressive and tensile strengths increase as the temperature of the rock specimen is lowered. His data show that adsorbed moisture plays a crucial role (Rehbinder effect) in altering the strength. Sellmann (1989) compiled a collection of unconfined compressive strength data, primarily from CRREL investigations, to show that the strengths of granite, sandstone, and limestone increase with cooling. However, these data were taken from quasi-static tests and are inadequate to predict the influence of strain rate under impact loading conditions.

In many mining operations, particularly in arctic mines, rock behavior during drilling, blasting or comminution processes is not sufficiently understood. This is because of the significant changes in properties due to low temperature and high strain rate. Kawatra and Eisele (1989) have reported serious degradation of efficiency in autogenous grinding process of an iron ore milling plant at low temperatures and attributed this to the temperature-dependent increase in rock strength. Using the Hopkinson bar technique over stress rates from 1.38×10^{-1} to 206.84 MPa s^{-1} (2×10^1 to 3×10^{10} psi s^{-1}), Kumar (1968) observed that the strengths of both basalt and granite increased dramatically (over 60%) at the lower temperatures. He concluded that, as with metals, increasing the stress rate or lowering the temperature has similar effects on rock strength, and that the mechanisms of rock fracture are thermally activated. However, tensile strength (not compressive strength) is the most fundamental parameter involved in consideration of rock fracture, and (to the authors' knowledge) to date, no work has been reported that shows the tensile strength behavior of rocks at low temperatures and high strain rates. Our interest in this report centered on tensile failure in intact rock specimens of disk shape resulting from diametral impact loading. Brazilian test specimens were used in a split Hopkinson bar test setup. Test results were compared with those obtained under quasi-static tests.

Stress solutions of diametral compression of disks were studied in 1883 by Hertz and more recently by Hondros (1959) and Colback (1966). Mellor and Hawkes (1971) have extensively discussed the application of these solutions to indirect tensile tests and particularly in determining uniaxial tensile strength for Griffith-type materials. They have shown that according to the Griffith criterion, the exact center of the disk is the only point at which the conditions for tensile failure at a value equal to the uniaxial strength are met. At other locations along the loading diameter, the stresses are sensitive to the angular distance a over which the load is applied (see Fig.1):

$$\sigma_\theta = +\frac{2P}{\pi D h}\left[\frac{\sin 2\alpha}{\alpha} - 1\right] \cong \frac{2P}{\pi D h} \tag{1a}$$

$$\sigma_r = -\frac{2P}{\pi D h}\left[\frac{\sin 2\alpha}{\alpha} + 1\right] \cong \frac{-6P}{\pi D h} \tag{1b}$$

(after Hondros 1959) where P is the applied load, D is the diameter and h is the thickness of the disk-shaped specimen. For $\alpha < 15°$, using these expressions will introduce only 2% error.
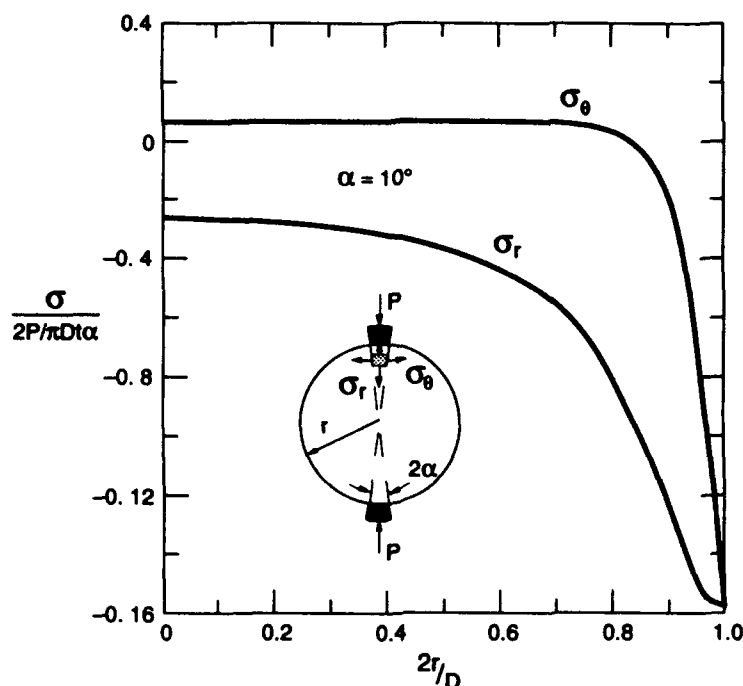
Figure 1. Distribution of stress along the loading diameter of a solid disk (after Hondros 1959).

EXPERIMENTAL PROCEDURES

Test materials

The two rocks chosen for the study were an Italian limestone and Barre granite. Barre granite is well characterized in rock mechanics literature. It has a small degree of anisotropy, the influence of which was ignored in the current tests. It contains about 27% quartz, 35% plagioclase feldspar, 20% microcline, and 16% mica. It has a porosity of about 0.08%, and the grain size around 0.76 mm (0.03 in.) (Peck et al. 1985). The Italian limestone was procured from a local monument stone manufacturer for its relative uniformity and small size of the grains, approximately 0.25 mm (0.01 in.), which ensure bulk homogeneity and representative behavior in small test specimens. Both rocks had the advantage of being strong enough to resist damage by experimental processing. The disk-shaped test specimens were cut from about 46.23-mm (1.82-in.)-diameter cores of each type of rocks into 19.81-mm (0.78-in.) nominal thickness.

Dynamic tests

One of the major reasons for the lack of understanding of the impact behavior of rocks is the difficulty in performing definitive experiments. There is difficulty first in producing well-defined and analyzable stress waveforms and, second, in subjecting the rock specimens to well-defined analyzable stress wave loads in an interpretable experiment. One suitable method to overcome these difficulties is to use the split Hopkinson-bar technique (Kolsky 1953). Compression testing of materials at low temperatures using this type of apparatus was reviewed in an earlier publication (Dutta et al. 1987). The apparatus used in the current investigation is identical to the compression apparatus but here the test specimens are subjected to diametral compression, so that the failure stresses are tensile (Brazilian test). The analysis of tensile test data obtained this way requires further examination. Therefore, a brief description of the experimental procedure is presented to provide a more complete background for this analysis.

A schematic of the test apparatus is shown in Figure 2. The apparatus consists of three 38.10-mm (1.5-in.)-diam. stainless steel bars, the striker bar, the incident bar, and the transmitter bar. To avoid generation of bending waves the last two bars are precisely aligned to the striker bar with a series of adjustable ball bearings. To run a test, the striker bar impacts against the incident bar, and generates a compressive stress wave in each bar that travels away from the impact face. The free end of the
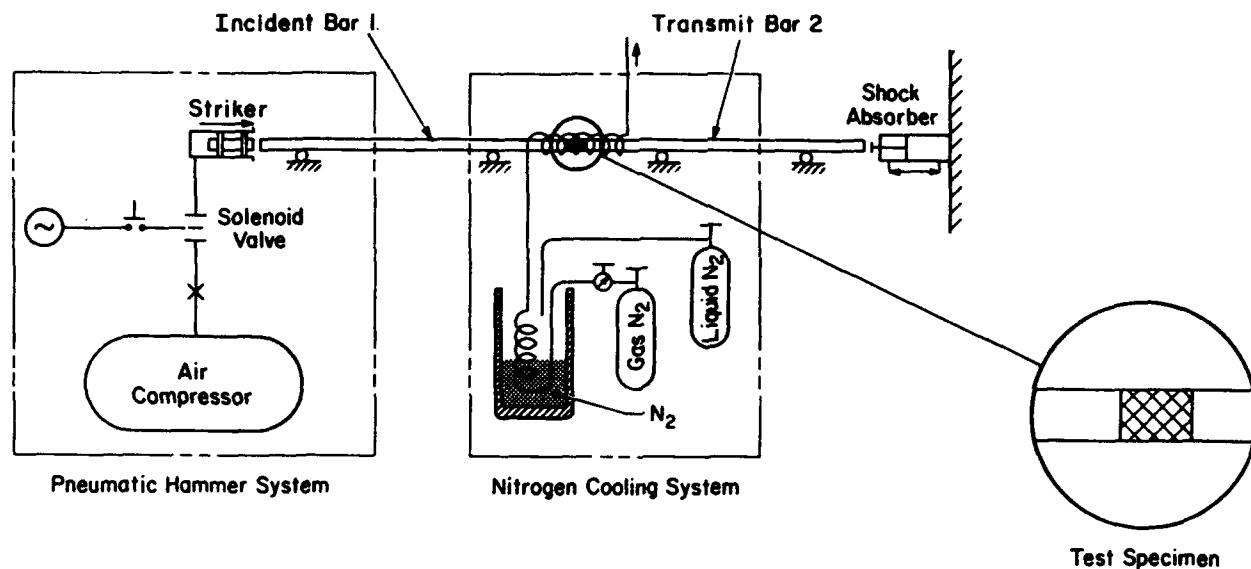
2

Figure 2. Schematic of the Hopkinson bar test setup for the Brazilian indirect tensile test.

striker bar reflects the compressive stress wave as a tensile stress wave, which upon reaching the impact face separates the striker from the incident bar. When the wave in the incident bar reaches the specimen, sandwiched between the incident and transmitter bar, a portion of the wave is reflected back into the incident bar. If no other energy is assumed to be lost, the rest of the wave is transmitted into the specimen. The wave travels through the specimen at its sound wave velocity until it reaches the transmitter bar. At this point again, a portion of the wave is reflected back into the specimen and the rest is transmitted into the transmitter bar. The deformation of the specimen under the impact stress is analyzed based on the assumption (Kolsky 1953) that the state of stress over the cross-sectional area of the pressure bars is one-dimensional. A departure from this assumption will make the wave front deviate from a plane to a curved front (nonuniform stress). This is overcome by having a slender diameter/length ratio < 1/50 (Zukas 1982) for the bars. In our test apparatus the slenderness ratio is 1/64. Results from a 500-kHz sonic pulse test show that the compression wave velocity for both rocks was of the order of 4272.2 m (14000 ft) s⁻¹ (Kalafut 1991). Because the wave has to travel only 46.23 mm (1.82 in.) (which is equal to the diameter of the specimen), the passage time of the wave front would be 10.7×10^{-6}s. The incident waveforms being about 160×10^{-6}s long would therefore establish a stress distri-

bution within the material equivalent to the static loading situation, as shown in Figure 1, through multiple reflections from the interfaces.

The mechanics of Hopkinson bar is simple and straightforward. Consideration of unidirectional plane wave propagation shows that the displacement u of a plane of the bar subjected to stress wave s given by

$$u = \frac{1}{\rho c} \int_0^t \sigma(t) \, dt \qquad (2)$$

where ρ = density of the bar
        c = longitudinal wave velocity
        $\sigma(t)$ = stress amplitude at any instant of time t from the beginning of the wave.

Thus, the interface displacement of the incident bar at the incident end of the specimen will be

$$u_i - u_r = \frac{1}{\rho c} \int_0^t [\sigma_i(t) - \sigma_r(t)] \, dt \qquad (3)$$

where the suffixes i, r and t relate to the incident, reflected and transmitted waves, and the interface displacement of the transmitter bar at the specimen's other end will be

$$u_t = \frac{1}{\rho c} \int_0^t \sigma_t(t) \, dt \qquad (4)$$

The total diametral deformation u_T of the disk

3

specimen will be the algebraic sum of displacements of the two interfaces. Thus

$$u_T = u_i - u_r - u_t$$

$$= \frac{1}{\rho c} \int_0^t \left[\sigma_i(t) - \sigma_r(t) - \sigma_t(t) \right] dt \qquad (5)$$

Equation 5 shows that the diametral deformation of the specimen disk is the function of stress levels in the incident and transmitter bars. These stresses are easily determined from the bar strain, measured with electric foil strain gauges, and the known Young's modulus E of the bar materials. It is, however, necessary to refer to these stresses from the same time reference base, usually taken at the incident bar/specimen interface. The average of the stress values of the bars is used to determine the force on the test specimen that caused deformation. Thus, the force on the specimen is given by

$$P = a \left[\sigma_i(t) + \sigma_r(t) + \sigma_t(t) \right] \qquad (6)$$

where a is the cross-sectional area of the bars. The maximum force P_{max} obtained from eq 6 can be used in eq 1a to obtain the high strain rate tensile strength (T_d) of the specimen:

$$T_d = \frac{2P_{max}}{\pi D h} \qquad (7)$$

where D is the diameter of the specimen and h is the thickness.

Since

$$\varepsilon = \frac{\sigma}{E}$$

we obtain

$$\varepsilon_\theta = \frac{2P}{\pi D E h} \qquad (8)$$

$$\dot{\varepsilon}_\theta = \frac{2}{\pi D E h} \frac{dP}{dt} . \qquad (9)$$

The fracture energy also can be obtained from the stress waveform measurement. From the elementary stress wave propagation theory applied to the Hopkinson-pressure bars it can be shown that the energy of the stress wave at any instant t after beginning of the wave is

$$U(t) = \frac{ac}{E} \int_0^t \sigma^2(t) \, dt \qquad (10)$$

where c is the longitudinal wave velocity in the bar. Since the energy absorbed in fracturing, $U_a(t)$, would be the difference between the energy of the incident wave $(U_i(t))$, and the sum of reflected $(U_r(t))$ and transmitted $(U_t(t))$ wave energies,

$$U_a(t) = U_i(t) - U_r(t) - U_t(t) . \qquad (11)$$

$$U_a(t) = \frac{ac}{E} \int_0^t \left[\sigma_i^2(t) - \sigma_r^2(t) - \sigma_t^2(t) \right] dt . \qquad (12)$$

As stated before, the tests were done with the disk samples held diametrically between the two horizontal pressure bars. A slight pressure by two rubber bands on the two bars held the specimens in position. For low-temperature tests an insulated chamber was used to control the sample temperature. The chamber was cooled by venting nitrogen gas chilled by liquid nitrogen as shown in Figure 2. The flow of the gas was controlled by observing the specimen's temperature with the thermocouples mounted near it. When the desired temperature was stable for about 15 minutes, the solenoid valve of the hammer system was triggered to allow the compressed air to drive the striker bar to impact on the incident bar. The strain gauges mounted at the midpoint of the 2.44 m (96-in.)-long bar recorded the stress waveforms (stress vs time) incident to and reflected from the specimen/bar interface. The trace 1 records in Figure 3 show these stress waveforms. The upper trace 1 is the record from the Italian limestone and the lower one is from the Barre granite tests. The wave velocity in the stainless steel bar is 5022 m (197,531 in.) s^{-1}. At this velocity it takes 243×10^{-6} s for the wave to reach the strain gauge located 1.22 m (48 in.) from the bar end after the impact. Point A locates this point on trace 1 where the incident wave begins. After another 243×10^{-6} s this wave arrives at the incident bar/specimen interface and instantly the reflected portion starts the return trip. Again after 243×10^{-6} s the incident bar strain gauge records this signal. Point B on trace 1 locates this point. Thus the waveform at point A is the incident wave and at point B is the reflected wave.

To ensure complete fracture but limit the unwanted excess energy, the degree of impact was adjusted by controlling the air pressure driving the striker bar. The striker bar was driven by 0.41 MPa (60-psi) air pressure for the weaker Italian limestone and 0.69 MPa (100-psi) air pressure for the stronger Barre granite. These impacts produced incident waves of about 86.18-MPa (12,500)
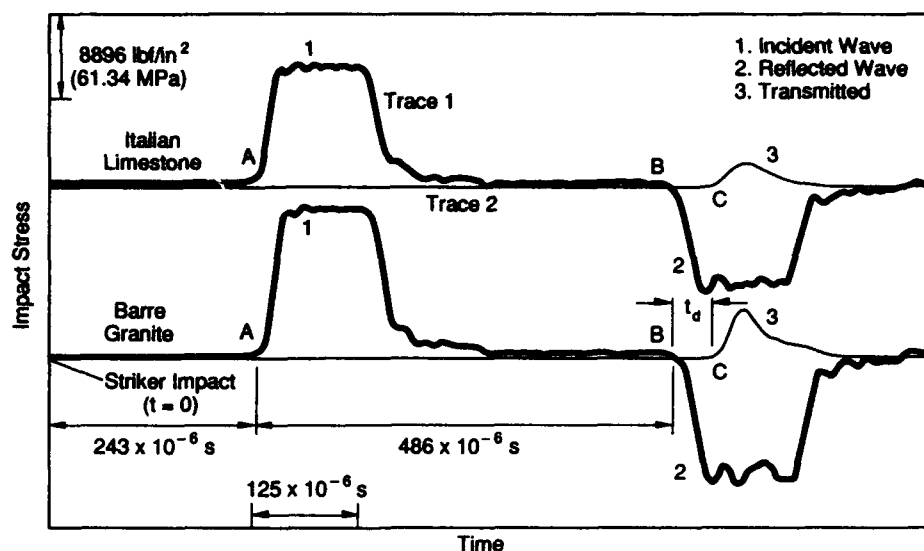
4

Figure 3. Typical stress waveform records from the Hopkinson bar tests.

and 113.76-MPa (16,500-psi) amplitudes respectively. Note that there is a noticeable difference in the shapes of the reflected waves; for both rocks the peaks of the reflected waves are jagged and lower than those of the incident waves. The reflected wave together with the transmitted wave is the result of the deformation and fracture development in the specimen. Its resultant shape (jaggedness) depends on the amount of energy expended at any instant of time from the incident wave. We assume that wave dispersion effects are negligible for such a short distance of travel.

The portion of the wave that remains after reflection continues to propagate through the specimen to the transmitter bar. If the stresses are lower than the elastic limit of the specimen, the specimen will simply deform elastically and after passage of the wave will regain its original dimension. In our tests the applied stress levels were higher than the strength of the specimens. Consequently, the specimens first deformed and finally broke when the diametral tensile stress exceeded the strength. The whole process takes a finite time, although very small, around 100×10^{-6} s. Thus the stresses reflected back to the incident bar and transmitted to the transmitter bar carry the history of the energy-transfer process to the rock specimen.

Figure 3 shows the two rocks' stress wave records from the transmitter bar as trace 2. These were picked up by the strain gauge located again 1.22 m (48-in.) from the bar/specimen interface. Points C on these traces are the arrival times of the

wavefronts. If there were no specimen at the interface and the bars were joined face to face, the arrival time of the wave from the interface to the gauge would be 243×10^{-6}s, which is exactly the same as that for the reflected wave from the interface. Under this condition the points B and C would be coincident on a vertical line of Figure 3. But, a finite time, t_d, elapsed as the wave passed through the specimen deforming it both elastically and plastically. The transmitted wave's amplitude is the maximum stress that could be sustained by the specimen before failure. Since the limestone is weaker than the granite, the amplitude of the transmitted wave for the limestone is smaller than that of the granite.

Quasi-static tests

Quasi-static tests were performed on the disk-shaped specimens of the Italian limestone and Barre granite both at room temperature (23°C) and low temperature (–30°C) with a servocontrolled hydraulic testing machine driving the loading platen at a speed of 0.254 mm (0.01 in.)/minute. An environmental chamber was used for all low temperature tests. As with the dynamic tests, this chamber was cooled with chilled nitrogen gas slowly vented through a regulating valve controlled by a temperature sensor near the test specimen. Tests were performed only when a stable temperature was established for about 15 minutes within the chamber. Load and displacement were recorded using the load cell and the LVDT trans-

5

ducers attached to the testing system, and the data were automatically transferred to the same digital data acquisition system as used for dynamic tests. The tensile failure stresses were then computed from the maximum load data using eq 1a.

TEST RESULTS AND DISCUSSION

A collection of representative specimens that failed under the dynamic and quasi-static tests is shown in Figure 4. Clearly there are multiple cracks along the fracture path in the dynamic test specimens and more fragments are formed, while in quasi-static tests only one major crack develops, thereby splitting the specimen in two. Thus, in dynamic fracturing the energy dissipation would be expected to be greater than in the quasi-static fracturing. No significant differences in the crack patterns are observed between room- and low-temperature fracturing.

The force vs. deformation curves presented in Figure 5 show a dramatic increase in stiffness and brittleness of both rocks in dynamic fracturing. The curves for the dynamic tests show that the load increased almost monotonically to a value A, which is slightly higher than the corresponding static strength, and then increased at a lesser rate to the peak value B. Possibly the failure started with the growth of incipient cracks at A and then was completed at B. Figure 6 shows a plot of force vs. time to failure. The time elapsed from A to B is of the order of 25×10^{-6}s for the granite and 40×10^{-6}s for the limestone. This indicates that, in the more brittle and stronger Barre granite, the crack propagation rate is faster than in the relatively weaker Italian limestone. The influence of
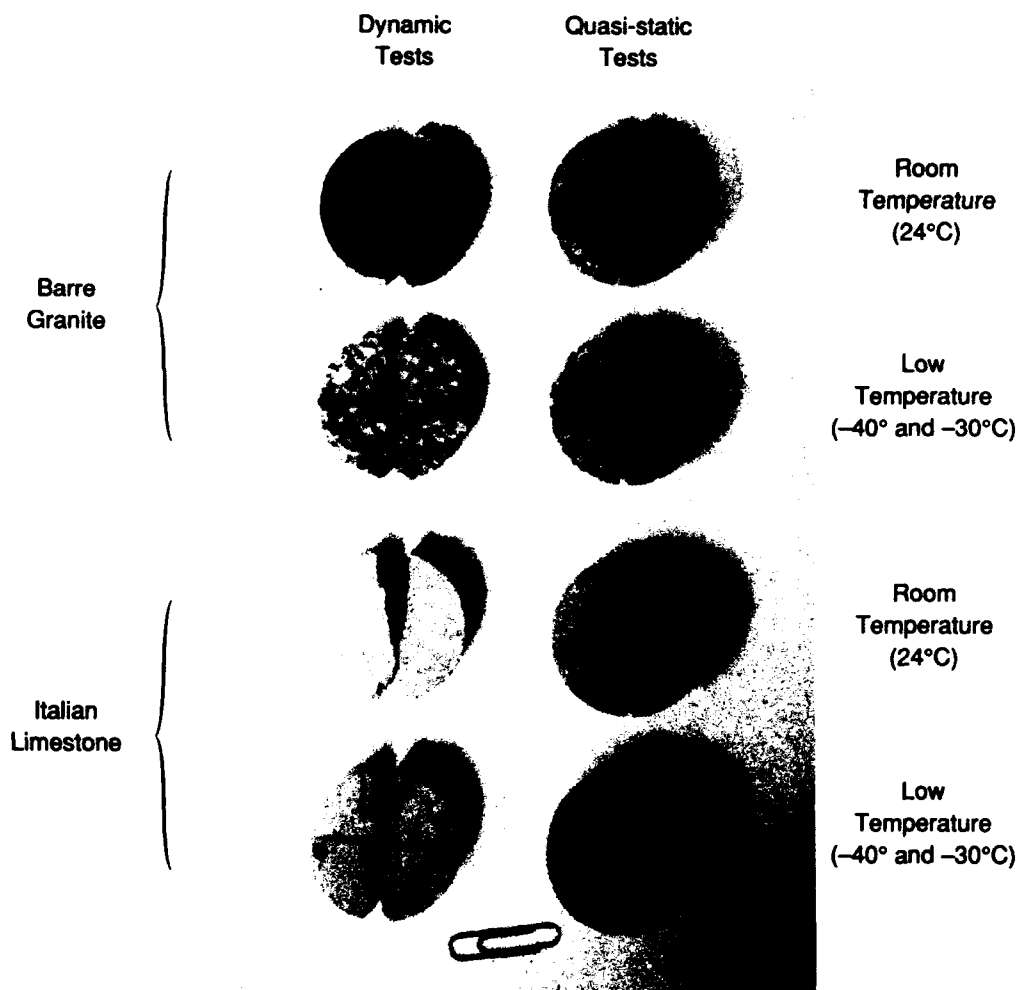

Figure 4. Failed specimens from quasi-static and dynamic Brazilian tests.
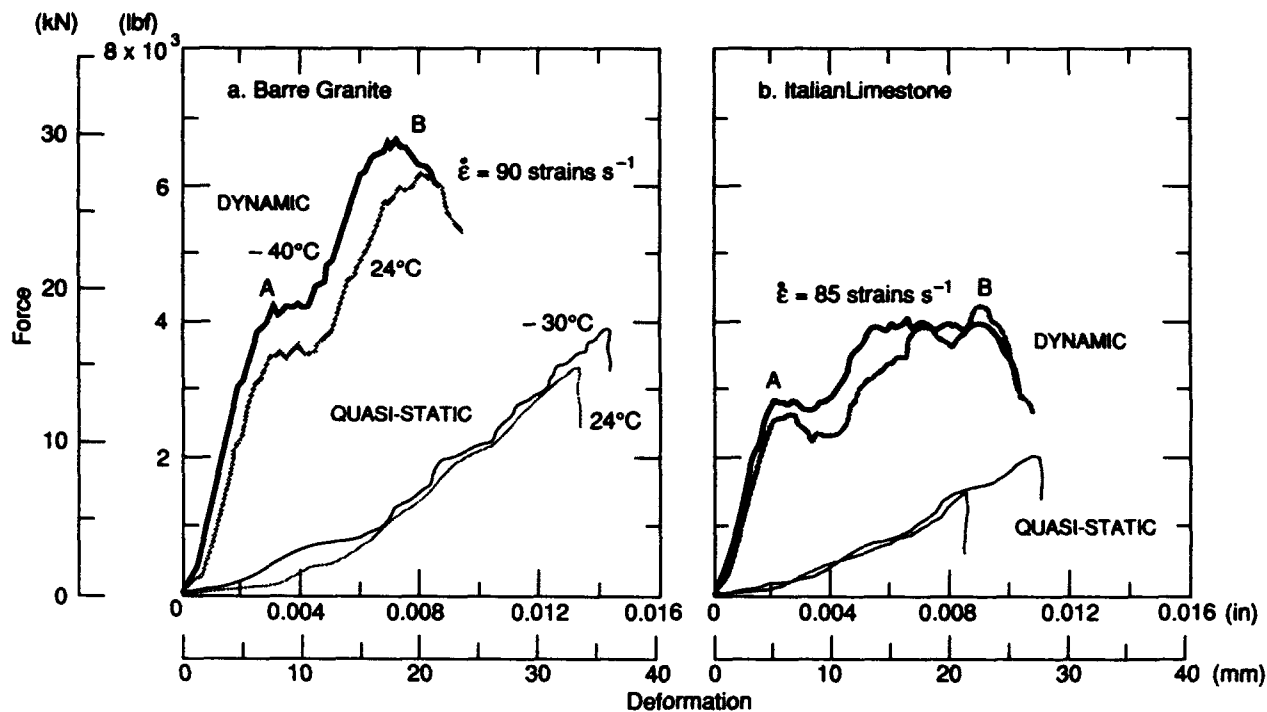
6

Figure 5. Force deformation behavior under quasi-static and dynamic loading at room and low temperatures.
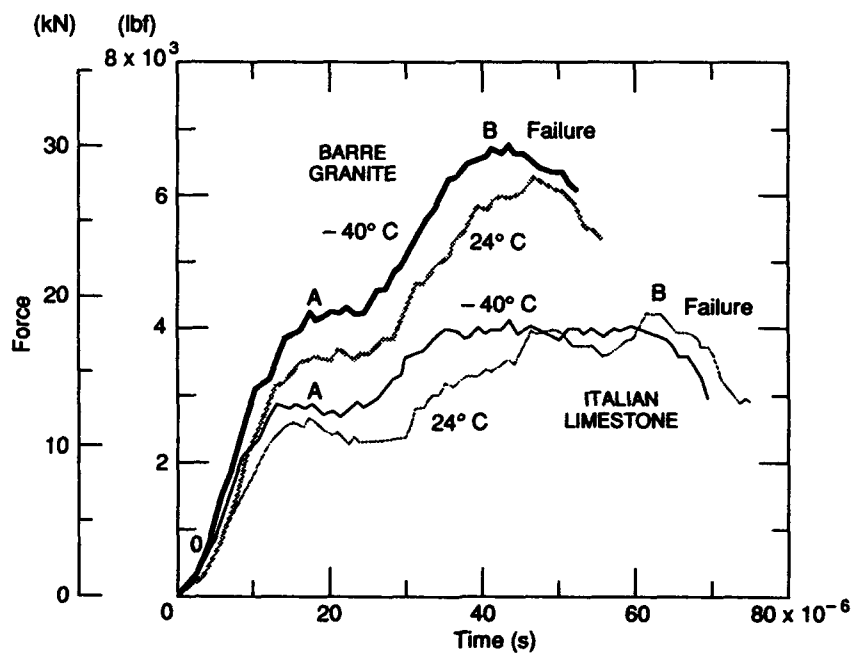

Figure 6. Force history of the Brazilian specimens in dynamic failure from Hopkinson bar tests.

7

Table 1. Tensile test results of the Italian limestone.

Specimen number	Temperature (°C)	Tensile strength MPa (psi)	Energy absorbed Joules (in.-lbf)
		Quasi-static tests	
L1	24.0	5.63 (817)	0.87 (7.7)
L2	24.0	5.38 (780)	0.73 (6.5)
L3	24.0	5.85 (849)	0.81 (7.2)
L4	24.0	5.35 (776)	0.73 (6.5)
L5	24.0	4.87 (706)	0.67 (5.9)
	Average	5.41 (785)	0.76 (6.7)
	Std. dev.	0.37 (53)	0.08 (0.7)
L6	–30.0	5.50 (798)	1.10 (9.7)
L7	–30.0	5.65 (819)	1.04 (9.2)
L8	–30.0	5.48 (795)	0.89 (7.9¬)
L9	–30.0	6.53 (947)	1.01 (8.9)
	Average	5.79 (840)	1.01 (8.9)
	Std. dev.	0.50 (72)	0.09 (0.8)
		Dynamic tests	
L10	24.0	12.87 (1866)	5.54 (49.0)
L11	24.0	11.28 (1636)	4.29 (38.0)
L12	24.0	11.91 (1727)	6.21 (55.0)
L13	24.0	11.92 (1729)	5.88 (52.0)
L14	24.0	11.31 (1641)	5.76 (51.0)
	Average	11.86 (1720)	5.54 (49.0)
	Std. dev.	0.64 (93)	0.79 (7.0)
L15	–40.0	13.07 (1896)	6.67 (59.0)
L16	–40.0	11.94 (1732)	5.88 (52.0)
L17	–40.0	11.43 (1658)	4.75 (42.0)
L18	–40.0	11.92 (1729)	5.31 (47.0)
L19	–40.0	12.47 (1809)	5.99 (53.0)
	Average	12.17 (1765)	5.76 (51.0)
	Std.dev.	0.63 (91)	0.68 (6.0)

temperature on crack propagation rate was not significant.

Other researchers (Stanturbano and Fairhurst 1991) have observed that not only the peak force, but the number of fragments also increases with higher impact velocities. From the dynamic tests the peak forces in Figure 5 and the multiple cracks in Figure 4 support these observations.

Lawn (1975) theorized that the number of fractures under an indentor is limited only by the mutual stress-relieving influence of neighbors. In stress wave loading of only a few tens of microsec-onds' duration, neighboring particles cannot move fast enough to cause stress relief. This results in the development of multiple cracks and fragments before final failure. As suggested by Stanturbano and Fairhurst (1991), these multiple fragments of rocks possibly provide the cushion beneath the impact surface causing the force to rise from A to the final failure point B.

All results of the tests are summarized in Table 1 for the Italian limestone and Table 2 for Barre granite. These data are illustrated graphically in Figure 7. It is immediately evident that there is a

8

Table 2. Tensile test results of Barre granite.

Specimen number	Temperature (°C)	Tensile strength MPa (psi)	Energy absorbed Joules (in.-lbf)
Quasi-static tests			
G1	24.0	12.44 (1804)	2.12 (18.8)
G2	24.0	10.89 (1580)	1.62 (14.3)
G3	24.0	11.43 (1657)	1.84 (16.3)
G4	24.0	12.27 (1780)	1.94 (17.2)
	Average	11.76 (1705)	1.90 (16.8)
	Std. dev.	0.72 (105)	0.20 (1.8)
G5	–30.0	14.13 (2050)	1.39 (12.3)
G6	–30.0	13.47 (1954)	2.20 (19.5)
G7	–30.0	12.74 (1847)	2.30 (20.4)
G8	–30.0	13.58 (1969)	2.63 (23.3)
	Average	13.48 (1955)	2.12 (18.8)
	Std. dev.	0.57 (83)	0.53 (4.7)
Dynamic tests			
G9	24.0	22.29 (3233)	11.07 (98.0)
G10	24.0	23.64 (3429)	10.51 (93.0)
G11	24.0	23.42 (3397)	11.75 (104.0)
G12	24.0	22.64 (3284)	10.85 (96.0)
	Average	23.00 (3336)	11.07 (98.0)
	Std. dev.	0.64 (93)	0.56 (5.0)
G13	–40.0	24.60 (3568)	11.07 (98.0)
G14	–40.0	23.18 (3362)	10.51 (93.0)
G15	–40.0	25.08 (3638)	11.75 (104.0)
	Average	24.29 (3523)	11.07 (98.0)
	Std.dev.	0.99 (143)	0.68 (6.0)

Note: Average tensile strain rates calculated as per eq. 9 in the dynamic tests for the Italian limestone were 85 strains s^{-1} and for Barre granite 90 strains s^{-1}.

dramatic difference in the strengths between the quasi-static and dynamic loading. For both rocks, the dynamic strength is almost twice that of the static strength, indicating that rock reacts quite differently to dynamic loading than to static loading. In particular, it is postulated that the fracture processes themselves are not the same under the two types of loading. Therefore, quasi-statically obtained values of tensile strength are probably of little value in predicting strength behavior under rapidly applied loading. The great increase in strength with increase in rate of loading probably results because, in failure under dynamic load, the weakest link in the rock may not necessarily have the time to participate in the fracturing process. The stress wave impact from the Hopkinson bar on the rock specimen is highly localized and the strength it measures is that of the rock only in this highly localized region. Under quasi-static loading, almost the total volume of the rock participates in the fracturing process so that the weakest element is likely to be the controlling factor.

Statistically, rock strength should be treated as a random variable instead of as a point estimate (i.e., mean strength and standard deviation). There
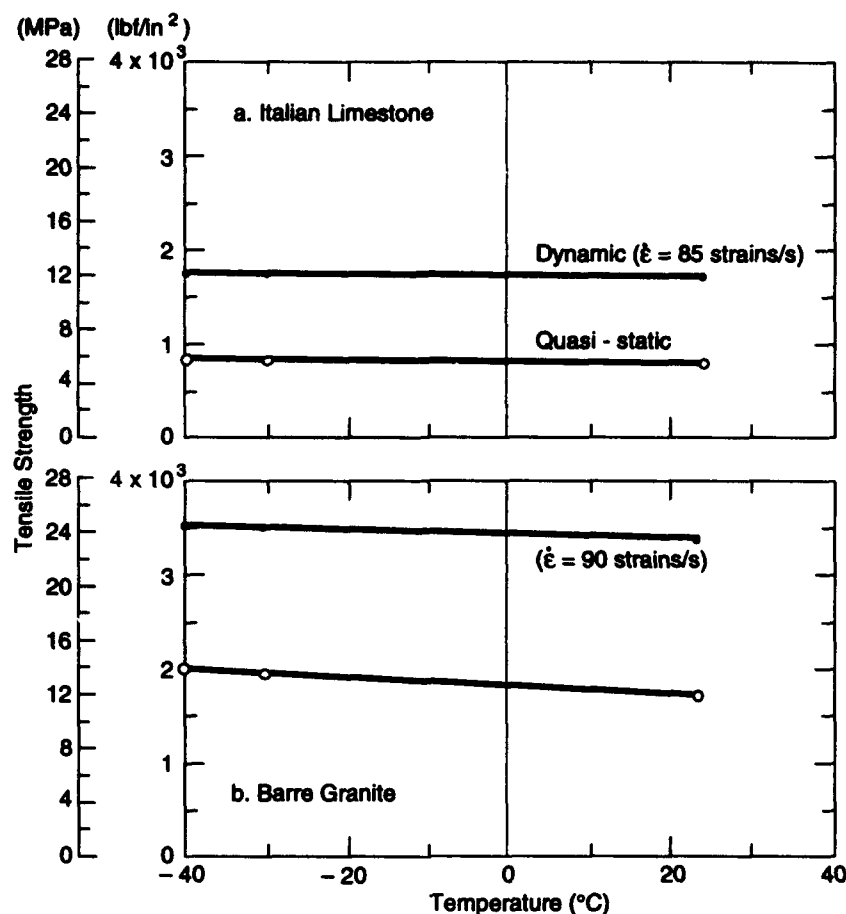
9

Figure 7. Effect of temperature and strain rate on the tensile strength.

are practical difficulties in determining the functional forms of probability distribution representing such properties. Considering the probabilistic nature of rock failure in light of the theory of extremes, and that failure occurs because the weakest of the homogeneously distributed flaws is the major determinant of strength, Yegulalp and Kim (1991) developed a model to forecast the strength of rocks as a function of size. As the dynamic fracturing process involves a complex interaction of multiple crack growth and cushioning by broken rocks, the weakest link theory would be difficult to apply directly and an alternative statistical approach may be required.

The influence of low temperature on the tensile strength is less dramatic. Tests were carried out over a temperature range of 24° to –30°C for quasi-static tests and 24° to –40°C for dynamic tests. The strength of Barre granite increased by 0.27%/°C or roughly 31.72 kPa (4.6 psi)/°C in quasi-static tests,

and 0.09%°C or roughly 20.0 kPa (2.9 psi)/°C in dynamic tests. Strength of the Italian limestone increased 0.13%/°C or about 6.9 kPa (1 psi)/°C in quasi-static and only 0.04%/°C or about 4.8 KPa (0.7 psi)/°C in dynamic loading. For normally dry rocks Mellor (1971) observed that the strength increases by roughly 0.2%/°C in the temperature range of 25 to –195°C. Since Mellor's data relate only to the quasi-static tests, our data for Barre granite are slightly higher and for the Italian limestone are slightly lower than Mellor's prediction. Mellor (1971) has shown that neither the thermal strain theory nor the thermally activated bulk processes (Kumar 1968) could satisfactorily explain the experimental observation of the strength increase, roughly 2×10^{-3} °C^{-1}. The possible explanation is that modification of water in the interior of the rock by temperature change is the dominant cause. The water in the rock interior may exist in absorbed or adsorbed state, or may occupy the

10

pores or interstitial spaces either partially or completely. As the temperature is lowered, thickness and mobility of the water in the rock interior are reduced, giving the effect of increasing strength, but there is as yet insufficient information to establish the precise mechanisms.

CONCLUSIONS AND RECOMMENDATIONS

Indirect tensile tests of an Italian limestone and Barre granite were conducted using the Hopkinson pressure bar for dynamic testing, and a servocontrolled hydraulic testing machine for quasi-static tests. Results show that the tensile strength and the deformability of these rocks are more sensitive to loading rate than the temperature. The mechanism of failure under dynamic loading by stress waves is significantly different from the quasi-static loading. Dynamic loading produces multiple fractures, absorbs more energy and, because it produces a cushion of broken rocks under the loading surface, requires higher loads for complete failure.

The influence of low temperature on strength and deformability under both static and dynamic loadings is less dramati.. Nevertheless, in all cases the strength increased with decreasing temperatures, possibly because of the immobilization of the interfacial water below freezing. But the precise mechanism is still unknown.

REFERENCES

Colback, P.S.B. (1966) An analysis of brittle fracture initiation and propagation in the Brazilian test. *Proceedings, First Congress of the International Society for Rock Mechanics*, Lisbon, 1966: 385–391.
Dutta, P.K., D. Farrell and J. Kalafut (1987) The CRREL Hopkinson bar apparatus. USA Cold Regions Research and Engineering Laboratory, Special Report 87-24.
Hondros, G. (1959) The evaluation of Poisson's ratio and the modulus of materials of low tensile resistance by the Brazilian (indirect tensile) test with particular reference to concrete. *Australian Journal of Applied Science*, 10: 243–268.

Kalafut, J. (1991) Pressure *(P)* wave velocity in Italian limestone and Barre granite. USA Cold Regions Research and Engineering Laboratory, Technical Note (unpublished).
Kawatra, S.K. and T.C. Eisele (1989) Effect of temperature on the performance of an autogeneous grinding circuit. *Advances in Autogeneous and Semiautogeneous Grinding Technology* (A.L. Mular and G.F. Agar, Eds.), Dept. of Mining and Mineral Process Engineering, University of British Columbia, Canada: 485–499.
Kolsky, H. (1953) Stress waves in solids. Oxford: Clarendon Press.
Kumar, A. (1968) The effect of stress rate and temperature on the strength of basalt and granite. *Geophysics*, 33: 501–510.
Lawn, B. (1975) Review. Indentation fracture: principles and applications. *Journal of Materials Science*, 10: 1049–1081.
Mellor, M. (1971) Strength and deformability of rocks at low temperatures. USA Cold Regions Research and Engineering Laboratory, Research Report 294.
Mellor, M. (1973) Mechanical properties of rocks at low temperatures. In Permafrost: The North American Contribution to the 2nd International Conference on Permafrost, Yakutsk, 13-28 July, Washington D.C.: Natural Academy of Sciences.
Mellor, M. and I. Hawkes (1971) Measurement of tensile strength by diametral compression of disks and annuli. *Engineering Geology*, 5: 173–225.
Peck, L., C.C. Barton and R.B. Gordon (1985) Microstructure and resistance of rock to tensile fracture. *Journal of Geophysical Research*, 90(B13): 11,533–11,546.
Stanturbano, R. and C. Fairhurst (1991) Fracture mechanics in the context of rock crushing. Preliminary experimental results concerning the impact of lime-stone spheres. *Rock Mechanics as a Multidisciplinary Science*, (J.-C. Roegiers, Ed.). Rotterdam: Balkema, pp 441–449.
Sellmann, P.V. (1989) Strength of soils and rocks at low temperatures. *Cold Regions Science and Technology*, 17: 189–190.
Yegulalp, T.M. and K. Kim (1991) Statistical assessment of scale effect on rock properties using the theory of extremes. SME-AIME 1992 meeting, Preprint No. 92.

REPORT DOCUMENTATION PAGE

Form Approved
OMB No. 0704-0188

1. AGENCY USE ONLY (Leave blank)	2. REPORT DATE October 1993	3. REPORT TYPE AND DATES COVERED

4. TITLE AND SUBTITLE

High-Strain-Rate Tensile Behavior of Sedimentary and Igneous Rocks at Low Temperatures

6. AUTHORS

Piyush K. Dutta and Kunsoo Kim

5. FUNDING NUMBERS

PE: 6.27.84A
PR: 4A762784AT42
TA: SS
WU: 019

7. PERFORMING ORGANIZATION NAME(S) AND ADDRESS(ES)

U.S. Army Cold Regions Research and Engineering Laboratory
72 Lyme Road
Hanover, N.H. 03755-1290

8. PERFORMING ORGANIZATION REPORT NUMBER

CRREL Report 93-16

9. SPONSORING/MONITORING AGENCY NAME(S) AND ADDRESS(ES)

Office of the Chief of Engineers
Washington, D.C. 20314-1000

10. SPONSORING/MONITORING AGENCY REPORT NUMBER

11. SUPPLEMENTARY NOTES

12a. DISTRIBUTION/AVAILABILITY STATEMENT

Approved for public release; distribution is unlimited.

Available from NTIS, Springfield, Virginia 22161.

12b. DISTRIBUTION CODE

13. ABSTRACT (*Maximum 200 words*)

The influence of low temperature on the stress–strain behavior, fracture strength, and energy absorption in the dynamic fracturing of a limestone and a granite was determined by experiments conducted with a special low temperature split-Hopkinson pressure bar in the tensile strain rate regime of 80–100 strains s^{-1}. The tensile strength was determined by diametral compression of disk samples (Brazilian method) at –40°C and 24°C. Diametral strains to failure were monitored with a high-speed digital oscilloscope to observe deformations at microsecond intervals. These data were then compared with the results from room and low temperature quasi-static tests. Results show that the tensile strength and the deformability of these rocks are more sensitive to loading rate than to temperature. The mechanism of failure under dynamic loading by stress waves is significantly different from that under quasi-static loading. Dynamic loading produces multiple fractures, absorbs more energy and, because of the cushion of broken rocks produced under the loading surface, requires higher loads for complete failure. The influence of low temperature on strength and deformability under both static and dynamic loadings is less dramatic. Nevertheless, in all cases the strength increased with decreasing temperatures, possibly because of the immobilization of the interfacial water below the freezing temperature.

14. SUBJECT TERMS	Cold regions engineering Deformability Fracture strength Granite	Limestone Stress–strain behavior Tensile strength	15. NUMBER OF PAGES 17
			16. PRICE CODE

17. SECURITY CLASSIFICATION OF REPORT	18. SECURITY CLASSIFICATION OF THIS PAGE	19. SECURITY CLASSIFICATION OF ABSTRACT	20. LIMITATION OF ABSTRACT
UNCLASSIFIED	UNCLASSIFIED	UNCLASSIFIED	UL